

Autoionization-Pumped Laser

J. Bokor

Bell Laboratories, Holmdel, New Jersey 07733

and

R. R. Freeman

Bell Laboratories, Murray Hill, New Jersey 07974

and

W. E. Cooke

Department of Physics, University of Southern California, Los Angeles, California 90007

(Received 12 February 1982)

Doubly excited autoionizing states in barium of the configuration $6p_{3/2}n p$ ($n \geq 12$) are shown to decay preferentially to yield the $6p_{1/2}$ excited state of Ba^+ . The resulting population inversion is used to produce amplified spontaneous emission at 493 and 650 nm corresponding to the $6p_{1/2}-6s_{1/2}$ and $6p_{1/2}-5d_{3/2}$ transitions in Ba^+ . This principle of selective autoionization is expected to be applicable to the construction of a new class of ion lasers extending into the vacuum-ultraviolet wavelength region.

PACS numbers: 32.80.Dz, 42.55.Hg

In general, when an atom is excited to an autoionizing state whose energy is greater than several of the atomic ionization limits all of the energetically possible final ion states are produced. The branching ratios to different final ion states are determined by the degree of configuration interaction coupling the ion-plus-bound-electron configuration to the various ion-plus-continuum-electron configurations. In certain cases, preferential decay to specific excited ionic states occurs. Such behavior has been identified in Ba ,¹⁻⁴ Yb ,³ Pb ,⁵ and Na .⁶ Gallagher and co-workers^{1,2} first pointed out that this effect might be useful in creating ionic population inversions resulting in laser action. We refer to this phenomenon as selective autoionization.

We report the first demonstration of laser action in an atomic ion pumped by selective autoionization. Amplified spontaneous emission (ASE) was observed on two visible transitions in Ba^+ following stepwise two-photon excitation of selected autoionizing states in neutral Ba . A schematic energy-level diagram showing the relevant barium states and optical transitions is shown in Fig. 1. The autoionizing states of interest are of the nominal configuration $6pnp$ and were excited via the $6snp$ resonant intermediate state. Ultraviolet laser radiation tunable near 247 nm was used for the first transition, $6s^2-6snp$, while visible laser radiation tunable near 455 nm was used to make the second transition, $6snp-6pnp$. Two Rydberg series of $6pnp$ autoionizing states exist, each converging to one

of the two spin-orbit-split $6p^2P_{1/2,3/2}$ levels in the ion (see Fig. 1). These two series are labeled as $6p_{1/2}n p$ and $6p_{3/2}n p$. States belonging to the $6p_{3/2}n p$ series with $n \geq 12$ lie above the $6p_{1/2}$ ion

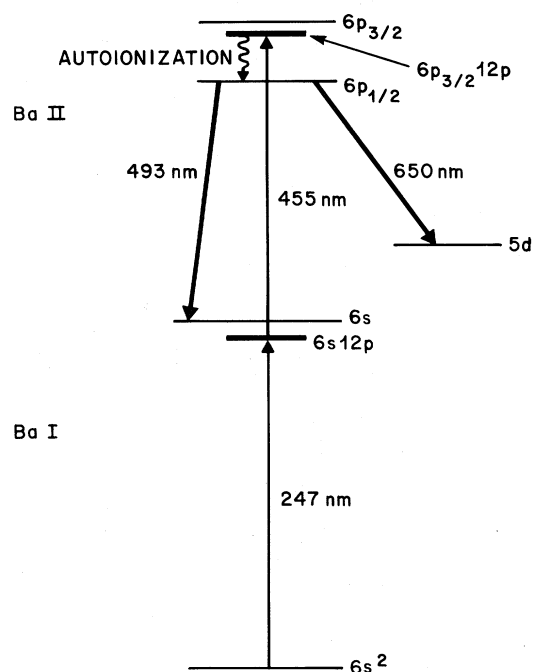


FIG. 1. Schematic energy-level diagram showing states of both neutral and singly ionized barium. The selective decay of the $6p_{3/2}12p$ autoionizing state to yield the $6p_{1/2}$ excited ionic state is shown as well as the optical transitions in Ba^+ which exhibited amplified spontaneous emission (ASE).

limit and were found to decay preferentially to $6p_{1/2}$ ions. Population inversion of the $6p_{1/2}$ ion level with respect to both lower-lying states in the ion ($6s$ and $5d$) was demonstrated in a Ba vapor cell by the observation of ASE at 493 and 650 nm corresponding to the $6p_{1/2}$ - $6s_{1/2}$ and $6p_{1/2}$ - $5d_{3/2}$ transitions, respectively.

In addition, spectroscopic investigations of the $6pnp$ states were performed in an atomic beam apparatus. Good correlation was found between the excitation spectrum for ASE found in the cell experiments and the ionization spectrum measured in the beam experiments. Linewidths for the $6p_{3/2}np$ ($n \geq 12$) states were found to be a factor of up to 17 times wider than the corresponding $6p_{1/2}np$ states. This behavior is qualitatively similar to that found for the $6pns$ states in barium^{1,2} and arises because these $6p_{3/2}nl$ states can decay into the newly opened $6p_{1/2}$ channel.

For the experiments reported here, ultraviolet radiation, tunable near 247 nm, was produced using a pulsed dye laser pumped by the second-harmonic output of a Nd-doped yttrium aluminum garnet laser and standard nonlinear optical techniques (second-harmonic generation and sum-frequency generation in potassium dihydrogen phosphate crystals). Up to 1-mJ pulses of 5 nsec duration were produced at 247 nm in a linewidth of 2 cm^{-1} at a repetition rate of 10 pulses/sec. Visible radiation, tunable near 450 nm, was derived from a second dye laser. Up to 10-mJ pulses of 5 nsec duration were produced in a linewidth of 0.5 cm^{-1} at 10 pulses/sec. The visible and ultraviolet beams were spatially and temporally overlapped and directed into either a Ba vapor cell or a Ba effusive atomic beam apparatus.

The atomic beam apparatus is similar in construction to that used by Gallagher, Safinya, and Cooke.¹ Total ionization yield spectra were taken by fixing the ultraviolet wavelength to the $6s^2^1S_0$ - $6snp^1P_1$ transition,⁷ and then scanning the visible wavelength laser in the vicinity of the $6s^2S_{1/2}$ - $6p^2P_{3/2}$ transition in Ba^+ . Doubly excited autoionizing states of the nominal configuration $6p_{3/2}np$ were thus excited. (However, as discussed below, the data indicate significant configuration mixing.) Both of the excitation lasers were well polarized and experiments were performed with the relative polarization either parallel or crossed. The selection rules are easily derived and show that with parallel polarization, only $J=0$ and $J=2$ states are excited, while for crossed polarization, only $J=1$ and

$J=2$ states are excited. In this way, it was possible to assign a value of total J for each state observed.

In Fig. 2 the ionization spectra for the $6p_{3/2}12p$ states are shown for both parallel and crossed polarizations. Our assignments of total J are also shown. Similar spectra were taken for $12 \leq n \leq 16$. The shape of the spectrum was strongly dependent on the input energy, showing saturation and broadening behavior. In all linewidth measurements, the visible laser was heavily attenuated in order to avoid saturation. For the same total J , the $6p_{3/2}np$ states were generally much broader than what was found for $6p_{1/2}np$ states. For example, we measured the width of the $6p_{1/2}12p$ $J=0$ state to be 2 cm^{-1} while the $6p_{3/2}12p$ state has a linewidth of 34 cm^{-1} . More typically, $6p_{3/2}np$ linewidths were 2 to 3 times the corresponding $6p_{1/2}np$ linewidths, while in certain cases the $6p_{3/2}np$ linewidths were comparable with the corresponding $6p_{1/2}np$ linewidths.

We attempted to predict these spectra using JK , jj , and intermediate-coupling schemes

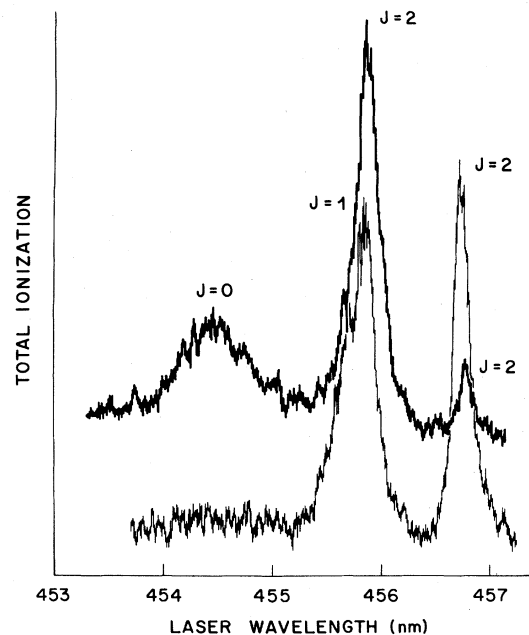


FIG. 2. Total ionization spectra for barium taken in an atomic beam apparatus. These data correspond to the nominal configuration $6p_{3/2}12p$. The upper, bold trace is the spectrum obtained using parallel laser polarizations. The lower, light trace was taken with orthogonal laser polarizations. The total angular momentum quantum number J is identified for each peak. The $J=1$ peak is a shoulder on the blue side of the central $J=2$ peak in the lower curve.

assuming a pure single configuration. No satisfactory predictions were obtained in this way, indicating the influence of configuration interaction. A multichannel quantum-defect theory (MQDT)⁸ analysis of the spectrum would therefore be desired. However, such an analysis requires additional spectroscopic data. For the purpose of simplicity, in the remainder of the discussion we will continue to use the single-configuration labels $6p, np$, bearing in mind that such a designation is an oversimplification.

The apparatus used in the cell experiments was 70 cm in length, sealed at both ends with LiF windows, and had a central hot zone of approximately 25 cm in length. Typical running conditions were at temperatures of 800–1000 C, with 20 to 50 Torr of argon used as a buffer gas. In most of the experiments, the ultraviolet radiation was set to excite the $6s^2\ ^1S_0-6s12p\ ^1P_1$ transition⁷ at $40\,428.7\text{ cm}^{-1}$. The visible radiation was then scanned, just as in the beam experiments. The ASE outputs were isolated from the input laser signals using either narrow-band interference filters or a 0.35-m monochromator. Both the 650- and 493-nm outputs were confirmed as due to ASE by three criteria. First, they exhibited threshold behavior either as a function of input pumping power with fixed vapor density or as a function of vapor density with fixed pumping power. Second, the outputs were well-defined, well-collimated beams. Third, approximately equal outputs were observed emerging from both ends of the cell. This last test was performed in order to eliminate coherent parametric interactions which would be phase matched in the forward direction only. The strongest output was observed at 650 nm, corresponding to the $6p\ ^2P_{1/2}-5d\ ^2D_{3/2}$ transition in Ba^+ . Using collimated input beams of approximately 0.05 cm^2 in area, with 0.5 mJ per pulse at 247 nm and 2.0 mJ per pulse at 455 nm, the 650-nm output which was copropagating with the input beams was measured to be $1\ \mu\text{J}$ per pulse. Both forward and backward outputs were also detected at 493 nm, corresponding to the $6p\ ^2P_{1/2}-6s\ ^2S_{1/2}$ transition in Ba^+ . The output energy at this wavelength was approximately 1 order of magnitude smaller than the output at 650 nm.

Figure 3 shows the excitation spectra for the 650-nm ASE output. At low input pumping power, the excitation spectrum is narrowed as a result of the highly nonlinear nature of the gain process. Threshold behavior is quite clearly shown in Fig. 3. The dependence of the 493-nm output on input

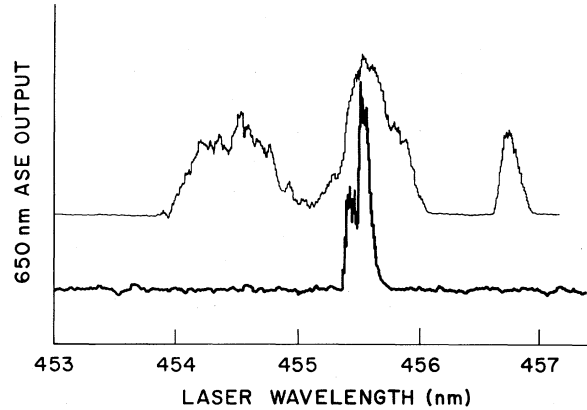


FIG. 3. Excitation spectra for the 650-nm ASE output taken in the cell experiments. The input laser polarizations were parallel for both curves. The lower, bold trace was taken with an input visible-laser pump power which was a factor of 10 lower than that used to obtain the upper, light trace.

power was qualitatively similar. The excitation spectra for both the 650- and 493-nm ASE outputs were also measured as a function of the relative polarization of the two pump lasers. The relative heights of the three main peaks were qualitatively similar to those found in the ionization spectra as shown in Fig. 2.

Selective autoionization behavior has been previously observed in several atomic systems via ejected electron spectroscopy.²⁻⁶ These systems all share the common feature that multiply excited states of the neutral atom which lie energetically between two spin-orbit-split excited ion limits are found to decay preferentially to the nearby ion level corresponding to the lower member of the doublet.²⁻⁶ Rosenberg, Lee, and Shirley³ have given a qualitative explanation for such preferential autoionization decay. A more rigorous analysis, involving an MQDT fit to the spectrum, would directly reveal the channel interactions and give the autoionization branching ratios. To our knowledge, MQDT has not yet been applied to the problem of predicting autoionization branching ratios.

Selective production of ion excited states by photoexcitation may also occur in regions of the continuum devoid of autoionizing states. Green and Falcone⁹ produced an inversion of the resonance line of Sr^+ by photoionizing a bound two-electron excited state of neutral Sr. In their experiment, the selectivity is achieved by radiatively coupling the bound excited state to the desired continuum. The well-known proposal of

Duguay and Rentzepis¹⁰ for pumping an x-ray laser by photoionization to selectively populate certain inner-shell vacancy states is based on similar principles. In selective autoionization, it is the dynamics of the two-electron interaction which leads to the selective decay of a doubly excited autoionizing state to the desired ion continuum. Selective autoionization thus represents a qualitatively new physical mechanism for the production of population inversions in ions. From a practical point of view, direct photoionization and selective autoionization are complementary in that the former is well matched to a broadband optical pumping source, while selective autoionization requires a relatively narrow-band pump source. Sources such as direct multiphoton laser excitation (as demonstrated here) and spontaneous anti-Stokes Raman scattering¹¹ might be used to pump new selective autoionization lasers.

In summary, selective autoionization has been demonstrated as a new physical principle for the production of population inversion and laser action in atomic ions. Since the phenomenon of selective autoionization has been observed in several inner-shell excited atoms²⁻⁶ it is believed to be quite general. We therefore anticipate the construction of a new class of optically excited ion lasers operating in the deep ultraviolet region

of the spectrum.

We wish to express our appreciation to R. H. Storz for his excellent technical assistance, and to T. F. Gallagher, C. Greene, S. E. Harris, and R. W. Falcone for discussions. This work was partially supported by the National Science Foundation under Grant No. PHY-7916444. One of us (W.E.C.) acknowledges the support of an Alfred P. Sloan Foundation Fellowship.

¹T. F. Gallagher, K. A. Safinya, and W. E. Cooke, *Phys. Rev. A* **21**, 148 (1980).

²W. E. Cooke and T. F. Gallagher, *Phys. Rev. Lett.* **41**, 1648 (1978).

³R. A. Rosenberg, S. T. Lee, and D. A. Shirley, *Phys. Rev. A* **21**, 132 (1980).

⁴J. P. Connerade and M. A. P. Martin, *J. Phys. B* **13**, L373 (1975); H. Hotop and D. Mahr, *J. Phys. B* **8**, L293 (1980).

⁵J. P. Connerade, *J. Phys. B* **14**, L141 (1981).

⁶E. Breukmann, B. Breukmann, W. Melhorn, and W. Schmitz, *J. Phys. B* **10**, 3135 (1977).

⁷J. A. Armstrong, J. J. Wynne, and P. Esherick, *J. Opt. Soc. Am.* **69**, 211 (1979).

⁸See e.g., U. Fano, *J. Opt. Soc. Am.* **65**, 979 (1975).

⁹W. R. Green and R. W. Falcone, *Opt. Lett.* **2**, 115 (1978).

¹⁰M. A. Duguay and P. M. Rentzepis, *Appl. Phys. Lett.* **10**, 350 (1967).

¹¹L. J. Zych, J. Lukasik, J. F. Young, and S. E. Harris, *Phys. Rev. Lett.* **40**, 1493 (1978).

Correlation and Relativistic Effects in Spin-Orbit Splitting

K.-N. Huang, Y.-K. Kim, and K. T. Cheng
Argonne National Laboratory, Argonne, Illinois 60439

and

J. P. Desclaux
Centre d'Études Nucléaires de Grenoble, F-38041 Grenoble, France

(Received 9 February 1982)

A large discrepancy between Dirac-Fock calculations and experiment for the spin-orbit splitting, ${}^2P_{1/2}$ - ${}^2P_{3/2}$, in the ground states of B- and F-like ions is resolved. The discrepancy arises from spurious terms which are inherent in the relativistic self-consistent-field procedure. Removal of these terms substantially improves the agreement between theory and experiment on spin-orbit splitting.

PACS numbers: 31.30.Jv

Forbidden transitions with wavelengths in the visible and uv region are of interest to astrophysics because they are convenient to study experimentally.¹ More recently, for the same reason, the magnetic dipole transitions between spin-orbit-split levels of highly stripped ions have be-

come an indispensable tool for plasma diagnostics in fusion devices.²

In a systematic study of energy levels for stripped ions, we noticed a large discrepancy between the Dirac-Fock calculations³ and experiment on the spin-orbit splitting, ${}^2P_{1/2}$ - ${}^2P_{3/2}$, in